communications biology

A Nature Portfolio journal

Article

https://doi.org/10.1038/s42003-025-07881-8

# Phylogenetic history and temperature adaptation contribute to structural and functional stability of proteins in marine mollusks



Xin-Lei Zhang[1,2], Ming-Ling Liao[1,2] ✉, Chao-Yi Ma[1,2], Lin-Xuan Ma[1,2], Qian-Wen Huang[1] & Yun-Wei Dong[1,2]

Teasing apart the influences of phylogenetic history from thermal adaptation is a focal challenge in understanding the factors driving change in protein stability. This study conducted comprehensive comparative analyses between the phylogenetic relationships and functional/structural stabilities at protein and mRNA levels of cytosolic malate dehydrogenase (cMDH) orthologs of 41 marine mollusks living at widely different environmental temperatures. At the protein level, a significant negative correlation between adaptation temperature and heat-induced movements of the cMDH backbone was found. The movement fluctuation of individual residue varied similarly among cMDH orthologs. At the mRNA level, the free energy that occurs during the formation of the ensemble of mRNA secondary structure was significantly positively correlated with adaptation temperature. The fraction of guanine and cytosine increased with adaptation temperature. The proportion of variance in adaptation temperature that can be explained by the thermal stability ($R^2$) was decreased after phylogenetic generalized least squares but was almost significant at both protein and mRNA levels ($P < 0.05$). Those analyses reveal the phylogenetic influence on the thermal adaptation of species. Our findings indicated that multi-level analysis of orthologous proteins should be considered alongside phylogenetic history to permit the development of a more comprehensive understanding of protein thermal adaptation.

Studying biochemical adaptation to widely different temperatures is a topic of broad interest from ecological, evolutionary, and conservation perspectives[1–5]. Many of these studies has focused on the adaptation of enzymes to temperature, including the trade-off between two fundamental properties, enzyme activity, and stability of higher-order structures[6–9]. The existence of the trade-off between structural stability and functional activity is crucial for organisms' survival and reproduction: stability must be high enough to allow retention of the native three-dimensional structure ("conformation"), yet not so high as to impede changes in conformation that are essential for function[3]. However, much remains to be elucidated about the evolution of this important structure-function relationship, notably its correlation to evolutionary history. To adequately resolve variation due strictly to adaptation to temperature, the phylogenetic effect on species' thermal tolerance traits over evolutionary timescales must also be taken into account[10–14]. Therefore, stability-function trade-offs in thermal adaptation should be considered alongside phylogenetic history, in order to help identify historical and eco-evolutionary processes that have shaped species' distributions and gain insights for predicting how the species will respond to future climate change[3,15].

Tolerances of species to high temperatures are largely conserved within lineages, i.e., similar values in thermal performance occur among closely related species[2,11,12,16,17]. A study of 60 species of marine snails whose habitat latitudes ranged from approximately 55°N (Robin Hoods Bay, England) to 35°S (Albany, Australia) showed that the thermal tolerance (indicated by the mean heat coma temperatures, HCTs) increased from low intertidal zone (only exposed during low tide) to high intertidal zone (only submerged at high tide). However, the thermal tolerance was significantly increased in mid-shore littorinoideans compared to littorinoidean snails living on low or

[1]Key Laboratory of Mariculture of Ministry of Education, College of Fisheries, Ocean University of China, Qingdao, China. [2]Shandong Key Laboratory of Green Mariculture and Smart Fishery, Fisheries College, Ocean University of China, Qingdao, China. ✉e-mail: liaoml@ouc.edu.cn

high intertidal zone[18]. A high phylogenetic conservation in thermal tolerance also exists in 94 Drosophila species from diverse climates[19]. These studies imply that the upper thermal tolerance limit is strongly influenced by phylogeny.

Warm-adapted enzymes exhibit distinct differences in both structure and function compared to cold-adapted orthologs. These variations in activity are not solely attributed to differences in stability; instead, they reflect evolution-driven enzyme dynamics, that is a trade-off between structural stability and flexibility[20]. Orthologous proteins of species that have evolved at different temperatures typically exhibit differences in thermal responses that reflect the protein's evolutionary thermal heritage[21,22]. For example, activity and stability profiles of 228 esterases and five extradiol dioxygenases from the marine microbiome in sediment and seawater metagenomes across 70 locations worldwide validate this thermal pattern: temperature-driven enzyme selection shapes microbiome thermal plasticity[22]. At the mRNA level, Park et al. described an anticorrelation between mRNA folding strength and protein evolutionary rate and demonstrated a prominent role of selection at the mRNA level in molecular evolution[23]. Further analysis of the temperature-adaptive stability of mRNA's secondary structure revealed a positive link between RNA's structural stability and thermal stability of the protein encoded by the mRNA[8]. Thus, the structural stability of both protein and mRNA are suitable tools for studying the phylogenetic pattern of thermal adaptation.

To explore the relative contributions of adaptation to specific thermal conditions versus phylogenetic history to the thermal tolerance of protein and mRNA homologs among species, we used cytosolic malate dehydrogenase (cMDH, EC 1.1.1.37) as our study system. As an essential enzyme in multiple metabolic pathways, cMDH orthologs have proven to be a powerful experimental system for elucidating adaptive patterns among orthologous proteins and analyzing how differences in amino acid sequence contribute to adaptive variation in function and structural stability[3]. Likewise, a study of the mRNAs of cMDH has revealed important aspects of the evolution of RNA stability[8]. The present study conducted a comprehensive comparative analysis between the phylogenetic relationships and functional/structural stabilities of the cMDH orthologs of 41 marine mollusks from 12 families with widely different habitat temperatures, ranging from lows of approximately 0 °C for Antarctic species to highs near 55 °C for tropical species. This wide range of evolutionary temperatures and a large number of study species allowed clarification of temperature-adaptive differences of both enzyme and mRNA orthologs. This study thus provides insights into the following issues: What are the main drivers of thermal structural stability of macromolecules in marine mollusks? Specifically, what are the roles of phylogenetic history versus temperature adaptation in governing the thermal responses of proteins and their mRNAs?

## Results

### Phylogenetic signals and environmental temperature regimes

The phylogenetic tree was constructed using the mitochondrial genomes from 41 marine mollusks (Fig. 1a). The orthologs from the families Neritidae (genus *Nerita*) and Littorinidae (genera *Littoraria*, *Littorina* and *Echinolittorina*) clustered on the same sub-branch, which indicated that the family Neritidae is closely related to the family Littorinidae in phylogeny. Similar patterns were found from the phylogenetic relationships of coding region sequences (CDSs) of 41 molluscan cMDH orthologs (Supplementary Fig. 1). In general, intertidal zones from high to low in the same latitude exhibit progressively lower environmental temperatures, and the macromolecules in marine mollusks living in the corresponding environment should possess a matching ability of thermal adaptation. However, in our study, we found that the thermal stability of cMDH orthologs (indexed by slope of ln residual activity (log transformed)) doesn't absolutely match the intertidal vertical distributions of species, as shown in the case of two species in the family Neritidae (Fig. 1). These species live in the middle intertidal but their cMDH orthologs are more heat-resistant than those of the family Littorinidae living in the high intertidal. This observation hints at an important role of phylogeny in setting macromolecular stability, and the environmental temperature is not the only factor shaping thermal adaptation.

The phylogenetic signal is the tendency for closely related species to resemble each other more closely in their biological characteristics than expected by chance[24]. Multiple indices have been developed to assess the degree of phylogenetic signal, such as Blomberg's $K$[25] and Moran's $I$[26]. Blomberg's $K$ value is calculated based on autocorrelation that considered as a statistical approach, and Moran's $I$ value is calculated based a model-based methods[27,28]. It is common to equate low phylogenetic signal with evolutionary lability. Similarly, strong phylogenetic signal has been interpreted as a sign of niche or evolutionary conservatism[29,30]. Blomberg's $K$[25] assumes a Brownian Motion (BM) model of trait evolution. A value close to zero indicates phylogenetic independence and a value of one indicates that species' traits are distributed as expected under BM. When $K$ value < 1 or >1, other models of trait evolution may effectively explain the data. The indices of structural stabilities of the cMDH orthologs tested in this study showed strong phylogenetic signals based on Blomberg's $K$ values ($K$-value > 0 and $P < 0.05$), except for the structural rigidity of protein (ΔRMSD) (Table 1). The $K$-values were 0.934 ($\Delta G_{fold}$), 0.416 (Slope of ln residual activity), 0.182 (Residues with ΔRMSF > 0.5 Å), 0.146 (Residues occurring in MRs with ΔRMSF > 0.5 Å), 1.266 (Fraction of G + C) and 0.110 (ΔRMSD). Moran's $I$ of each index showed similar patterns as Blomberg's $K$; the thermal stability of mRNA of the cMDH orthologs exhibited the strongest phylogenetic conservatism (Table 1). One clear way that trait evolution may differ from simple Brownian motion is if adaptation to a specific environmental factor occurs in some, but not all members of a group of species. At this point, the accuracy of Blomberg's $K$ will no longer be reliable[25]. We also examined the phylogenetic signals for different indexes of functional/structural stabilities of the cMDH orthologs of mollusks from different intertidal positions. The mollusks from different intertidal positions show similar patterns to the results for the 41 marine mollusks (Supplementary Table 1).

The differences in present environmental temperature were found among families in these 41 species of marine mollusks (Fig. 2). Due to the complex and variable environment of the intertidal zone, we chose representative temperature indicators to allow interspecies comparisons. The maximal body temperatures were extracted using a heat budget model (HBM) that incorporates comprehensive biological morphological characteristics and hourly tidal height data, to represent the corresponding environmental temperatures of mollusks that live in the splash zone, high and middle intertidal zone. The maximal sea surface temperatures (SSTs) were extracted as the representative environmental temperature of low-intertidal species. The maximal water temperatures at a depth of 1150 m were chosen to represent the environmental temperature of the deep-sea mussel. The present environmental temperatures (indicated by the 95$^{th}$ percentile of environmental temperature of respective habitats) were 39.70–42.96 °C (Neritidae), 35.62–43.71 °C (Littorinidae), 29.95–44.80 °C (Lottiidae), 26.52–43.25 °C (Tegulidae), 26.52–31.19 °C (Haliotidae), 43.74 °C (Trochidae), 28.44–35.46 °C (Mytilidae), 29.37 °C (Mactridae), 27.51–31.02 °C (Veneridae), and 28.47–31.19 °C (Arcidae), 8.36 °C (Laternulidae), and 11.01 °C (Pectinidae), respectively (Fig. 2b and Supplementary Table 2).

### Temperature-correlated differences in thermal stability of cMDHs

The relationship between the present environmental temperature (indexed by the maximum of the 2000−2014 monthly mean temperature 95th percentile) and the thermal stability (indexed by the slope of ln residual activity (log transformed)) of cMDH orthologs was analyzed (Fig. 3). A previous study showed that species living in the warmest habitats have the most thermally stable enzymes[7]. Whether or not PGLS analyses were used, the thermal stability of cMDHs was positively correlated with species' present environmental temperatures (Fig. 3a; without PGLS correction, $R^2 = 0.38$, $P < 0.001$; with PGLS correction, $R^2 = 0.21$, $P = 0.003$). The slope of ln residual activity after log-transformed of cMDHs of Neritidae (3.20) was significantly greater than these of Lottiidae, Tegulidae, Haliotidae,

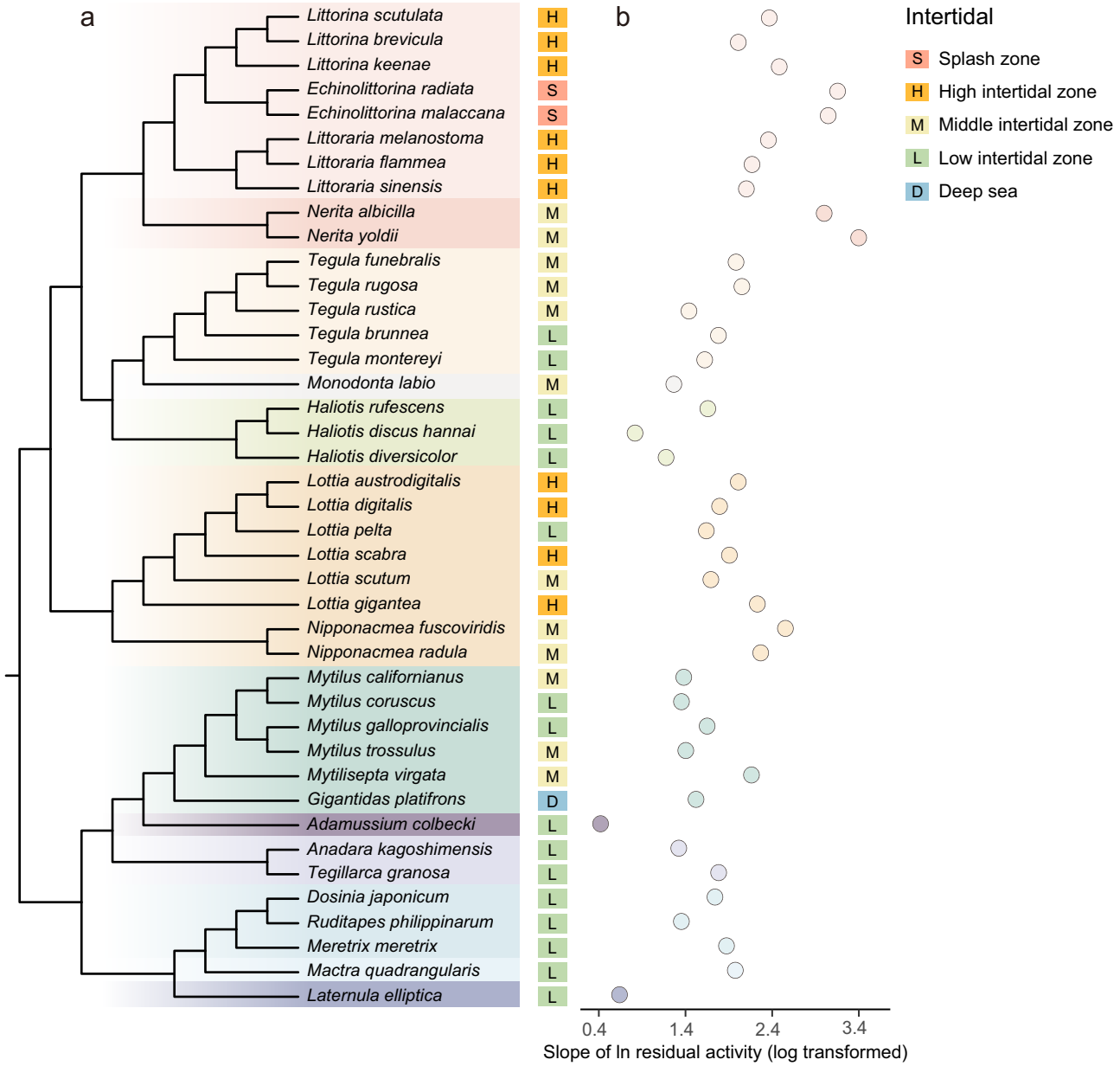


**Fig. 1 | Phylogenetic relationships of 41 marine mollusks and the corresponding thermal stability of their cMDH orthologs. a** A phylogenetic tree was constructed by referring to existing studies[44,71–75], and *Tegula*, *Lottia* and *Monodonta labio* lacked relevant research content, the COI sequences were used to supplement them. The intertidal vertical distributions of species are indicated (S: Splash zone; H: High intertidal zone; M: Middle intertidal zone; L: Low intertidal zone; D: Deep-sea). **b** Thermal stability of cMDH orthologs (indexed by slope of ln residual activity) from 41 marine mollusks. Data were log-transformed (base 10 logarithm) before the analysis using log-modulus transformation.

Mytilidae, Veneridae, and Arcidae (2.01, 1.78, 1.22, 1.58, 1.66, and 1.55, respectively), implying cMDHs of the species of families Neritidae has significantly higher thermal stability than orthologs species of other families (Fig. 3b, $P < 0.05$).

Molecular dynamic simulation (MDS) can provide further insights into how thermal stability varies among orthologous proteins and among different regions of a protein[7]. Our criterion for quantifying flexibility was the amount of change (measured in angstroms) in movement throughout the entire backbone atoms of protein (RMSD) and by individual amino acid residue (RMSF) that occurs when temperature is increased (Fig. 4 and Supplementary Table 3). RMSD generally refers to the structural deviation of the entire atomic backbone compared to a reference conformation at a specific moment, reflecting the structural rigidity of the protein; RMSF examines the structural change of a single residue over time in relation to the reference conformation, reflecting the flexibility of the residue. A larger RMSD value indicates the presence of a larger conformational change of the entire protein, and a higher RMSF value indicates a greater conformational flexibility for a given residue. The increase in RMSD (ΔRMSD) when the simulation temperature was increased from 15 to 42 °C was inversely related to the species' adaptation temperature (indexed by the slope of ln residual activity (log transformed)) (Fig. 4a; without PGLS correction, $R^2 = 0.31$, $P < 0.001$; with PGLS correction, $R^2 = 0.028$, $P = 0.296$). Lower values of ΔRMSD thus are found with proteins having more stable conformations and a higher resistance of conformation to thermal perturbation.

The numbers of residues showing a ΔRMSF greater than 0.5 Å were used to index the structural flexibility of a cMDH ortholog, whether in the overall sequence or in "mobile regions (MR)" that undergo marked changes in conformation during function (MRs: residues 90–105 in MR1 and residues 230–245 in MR2 of cMDH). Our previous study demonstrated that heat-induced ΔRMSF values across the overall sequence and, especially in

**Table 1 | Phylogenetic signals for different indexes of functional/structural stabilities of the cMDH orthologs based on the phylogenetic tree of 41 marine mollusks[a]**

| Index | *K*-value | *I*-value |
|---|---|---|
| Slope of ln residual activity | 0.416*** | 0.119* |
| ΔRMSD | 0.110 | 0.150** |
| Residues with ΔRMSF >0.5 Å | 0.182** | 0.173** |
| Residues occurring in MRs with ΔRMSF >0.5 Å | 0.146* | 0.121** |
| $\Delta G_{fold}$ | 0.934*** | 0.405*** |
| Fraction of GC | 1.266*** | 0.410*** |

Results are Blomberg's *K* and Moran's *I* values. Value > 0 and $P < 0.05$ represent the significant phylogenetic signal for the corresponding indexes of functional/structural stabilities of the cMDH orthologs. The thermal stability of enzyme (Slope of ln residual activity), structural rigidity of protein (ΔRMSD), structural flexibility of overall protein (Residues with ΔRMSF > 0.5 Å), structural flexibility of mobile regions (Residues occurring in MRs with ΔRMSF > 0.5 Å) and stability of mRNA ($\Delta G_{fold}$ and Fraction of GC) were used as indexes of functional/structural stabilities of the cMDH orthologs.
[a]The strength of phylogenetic signal with significance level: *$P < 0.05$; **$P < 0.01$, ***$P < 0.001$.

MRs were lowest in warm-adapted species, yet the sequence of MRs is highly conserved, likely because of the critical roles of the MR regions in protein functions like ligand binding and catalysis[7]. The number of residues for which ΔRMSF > 0.5 Å showed a negative correlation with the species' adaptation temperature (indexed by the slope of ln residual activity (log transformed)) (Fig. 4b: without PGLS correction, $R^2 = 0.35$, $P < 0.001$; Fig. 4c: without PGLS correction, $R^2 = 0.30$, $P < 0.001$). Using the PGLS analyses to eliminate the potential influence of phylogenetic effects, the correlation between thermal stability and flexibility of cMDHs was reduced but still significant (Fig. 4b: with PGLS correction, $R^2 = 0.22$, $P = 0.002$; Fig. 4c: with PGLS correction, $R^2 = 0.12$, $P = 0.025$).

The results of $T_m$ are consistent with that of the ΔRMSD to characterize the structural stability of cMDH orthologs (Supplementary Fig. 2). Restricted by the small sample size, the *P*-value in the regression analysis is not less than 0.05, but possesses a high degree of fit ($R^2 = 0.79$). The values of $T_m$ were 61.76 °C (*E. malaccana*), 62.84 °C (*E. radiata*), 62.21 °C (*L. keenae*), and 49.24 °C (*M. galloprovincialis*).

### Adaptive changes in stability of cMDH mRNA secondary structures

The free energy of formation ($\Delta G_{fold}$; kcal/mol) of each secondary structure ensemble of cMDH mRNA was simulated at a temperature of 37 °C. These analyses allowed evaluation of the relationship between the structural stabilities of the cMDH mRNAs and species' adaptation temperature (Fig. 5). $\Delta G_{fold}$ was negative for all mRNA orthologs, and the absolute values of $\Delta G_{fold}$ were significantly positively correlated with species' adaptation temperatures (indexed by the slope of ln residual activity (log transformed)) (Fig. 5a; without PGLS correction, $R^2 = 0.22$, $P = 0.001$; with PGLS correction, $R^2 = 0.23$, $P = 0.002$). The absolute values of log-transformed $\Delta G_{fold}$ of cMDHs of families Neritidae, Littorinidae, Lottiidae, Tegulidae, Haliotidae, Mytilidae, Veneridae, Arcidae were 2.56, 2.51, 2.39, 2.47, 2.46, 2.39, 2.42, and 2.36, respectively (Fig. 5c). The species of families Neritidae and Littorinidae have significantly greater structural stabilities of the cMDH mRNAs than those of families Tegulidae, Haliotidae, Veneridae, Mytilidae, Lottiidae, and Arcidae (Fig. 5c, $P < 0.05$).

To further elucidate adaptive changes in the stability of cMDH mRNA secondary structures, we compared features of the orthologous mRNAs that could potentially influence the stability of secondary structure: G + C content. The values of the log-transformed fraction of G + C were significantly positively correlated with the species' adaptation temperatures (indexed by the slope of ln residual activity (log transformed)) (Fig. 5b; without PGLS correction, $R^2 = 0.16$, $P = 0.011$; with PGLS correction, $R^2 = 0.18$, $P = 0.006$). The fraction of G + C values (log-transformed) of cMDHs of families Neritidae, Littorinidae, Lottiidae, Tegulidae, Haliotidae, Mytilidae, Veneridae, and Arcidae were −0.23, −0.27, −0.38, −0.30, −0.30, −0.40, −0.37, and −0.40, respectively (Fig. 5d). The cMDH mRNAs from species of families Neritidae and Littorinidae have significantly higher fraction of G + C (log transformed) than those of families Haliotidae, Laternulidae, Trochidae, Veneridae, Mytilidae, Mactridae, Lottiidae, and Arcidae (Fig. 5d, $P < 0.05$). Fraction of G + C (log-transformed) showed similar patterns as $\Delta G_{fold}$ values of cMDH mRNAs from families Neritidae, Littorinidae, Lottiidae, Tegulidae, Haliotidae, Mytilidae, Veneridae, and Arcidae.

### The combined role of evolutionary history and temperature adaptation

To further analyze the combined role of evolutionary history and environmental temperature in shaping the thermal adaptation of cMDH, the PGLS analyses were conducted to account for the potential influence of phylogenetic effects, indicating the extent to which phylogeny is affecting the error structure of the data[31]. Whether or not PGLS analyses were used to remove the effect of phylogeny, all the correlations we were concerned with remained significant (except for the structural rigidity of protein (ΔRMSD)), but the coefficient of determination ($R^2$) were decreased (Figs. 3–5). Those results show that the role of phylogeny in shaping interspecific variation of thermal adaptation in cMDH is significant, but not unique; the temperature adaptation plays a joint role.

### Neritidae and Littorinidae have the highest structural stabilities of the cMDH mRNAs

The results of MDS and mRNA secondary structure prediction showed that the cMDH orthologs of Neritidae and Littorinidae had the highest thermal structural stability (Figs. 3–5). To further illuminate this prominent difference, a cluster analysis algorithm called Two-Step Clustering was conducted using the data of the thermal stability, ΔRMSD, $\Delta G_{fold}$, and fraction of G + C of all orthologs from all 41 species studied. Consistent with our expected results, all species were clustered into two groups (Fig. 6a, Supplementary Table 4). Species in the families Neritidae and Littorinidae can be allocated into group 1; they have significantly higher thermal stabilities (indexed by the slope of ln residual activity (log transformed)) of cMDHs than those of others (Fig. 6b, $P < 0.01$). The values of ΔRMSD of cMDHs of group 1 and group 2 were 0.17 and 0.36, respectively, indicating the species of families Neritidae and Littorinidae have significantly greater global structural stabilities of the cMDH orthologs than those of group 2 (Fig. 6c, $P < 0.001$). The number of residues with ΔRMSF > 0.5 Å, and the number of residues occurring in MRs with ΔRMSF > 0.5 Å of cMDH of group 1 and group 2 were 33.3, 6.8, and 73.65, 17.03, respectively (Fig. 6d, e, $P < 0.001$), indicating the species of families Neritidae and Littorinidae have significantly lower conformational flexibility of the cMDH orthologs than those of group 2. The absolute values of log-transformed $\Delta G_{fold}$ values of cMDH mRNA orthologs in group 1 (2.52) are significantly higher than that in group 2 (2.42), indicating the species of group 1 possess significantly higher structural stabilities of the cMDH mRNAs than those of group 2 (Fig. 6f, $P < 0.001$). The fraction of G + C (log-transformed) of cMDH mRNA orthologs in group 1 (−0.26) is significantly higher than that in group 2 (−0.36), indicating the species of group 1 possess significantly higher structural stabilities of the cMDH mRNAs than those of group 2 (Fig. 6g, $P < 0.001$).

## Discussion

In the present study, we describe consistent patterns of convergent evolution in global and localized thermal structural stability at the protein and mRNA levels of cMDH orthologs from differently thermally adapted marine mollusks. Species of the families Neritidae and Littorinidae have much higher thermal stabilities of cMDH orthologs than those of the other families. Further analyses reveal that the families Neritidae and Littorinidae have a close phylogenetic relationship, and their cMDH orthologs exhibited high structural stability at both protein and mRNA levels, indicating the undeniable role of phylogenetic history in limiting thermal adaptation, especially the upper thermal limit. Comprehensive analyses of structural

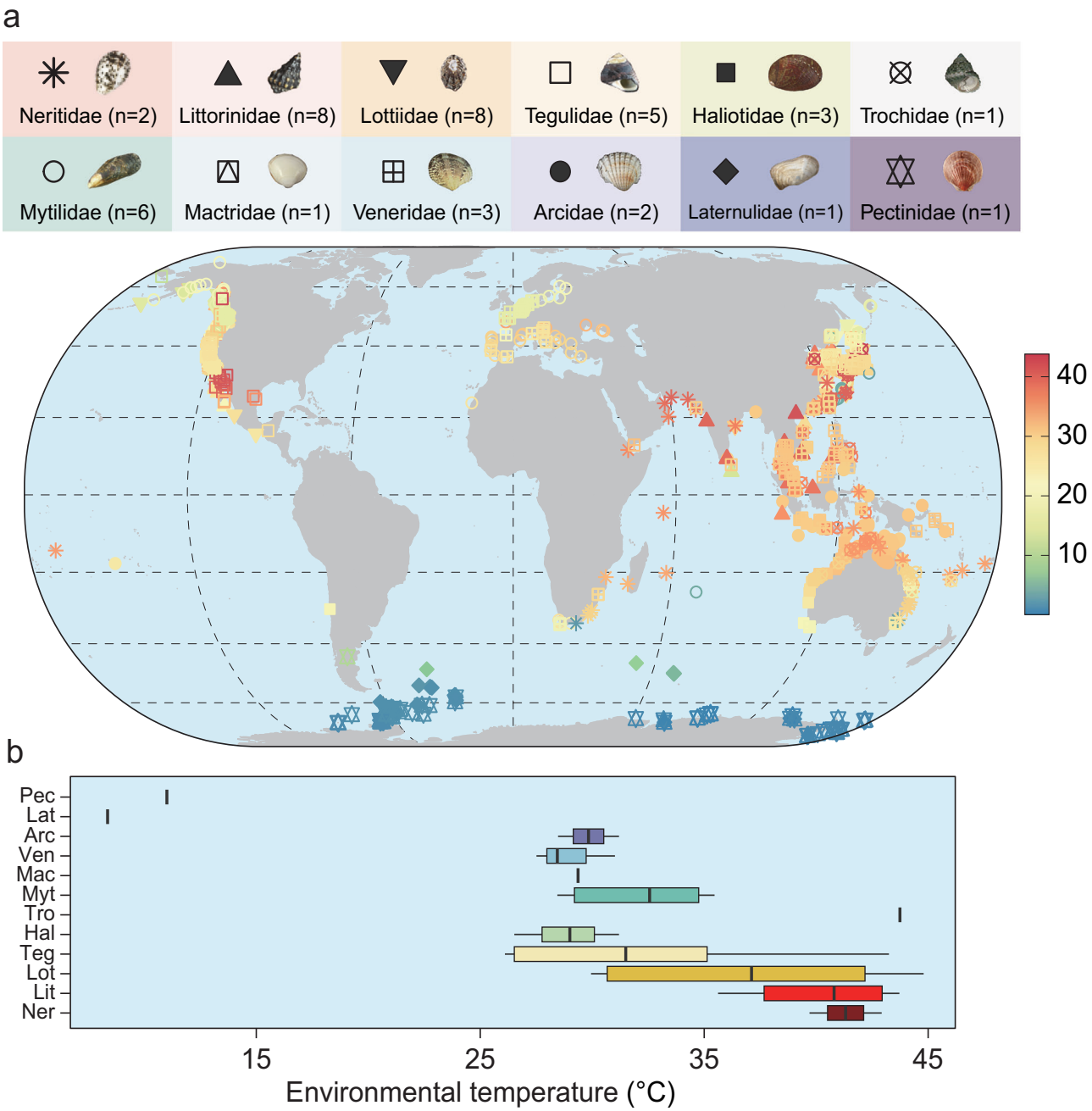


**Fig. 2 | Geographic distribution and environmental temperature of forty-one marine mollusks. a** Global distributions of the studied marine mollusks. Occurrence data were collected from Global Biodiversity Information Facility (GBIF). The plot symbol was colored to illustrate each location's 95th percentile of maximal environmental temperature. The number of the studied species in each family is indicated. **b** The ranges of the 95th percentile of maximal environmental temperatures from marine mollusks in the twelve families.

stability and phylogenetic relationships in cMDH orthologs from marine mollusks confirm the influence of thermal history on the thermal adaptation of different protein orthologs and offer insights into protein evolvability.

### Influence of phylogenetic history on thermal adaptation of proteins

Organisms' thermal tolerance is partly phylogeny dependent[10–14] and partly environmental temperature dependent[7,32,33]. Our phylogenetic independence analysis confirmed that the structural stabilities in cMDH orthologs from 41 marine mollusks are strongly influenced by evolutionary history (Blomberg's *K* and Moran's *I* values in Table 1). The PGLS analysis emphasized the combined role of evolutionary history and temperature adaptation in shaping the thermal tolerance of cMDH.

Proteins can maintain high stability and catalytic activity in a mild environment at the same time[34,35]. This indicates that the selection of thermal adaptation by the environmental temperature could be indirect, that is, the temperature first makes a selection for catalytic activity and thus affects structural stability. For example, a thermophilic enzyme must evolve increased catalytic activity at lower temperatures when encountering cooler environments, while accommodating relaxed selection on thermostability[34]. In other words, the conformational change of protein tends to maintain its original structural state rather than form a new stability on the premise of meeting the needs of catalytic activity to adapt to new environmental temperatures. This is essentially a consequence of Anfinsen's thermodynamic hypothesis that the native structure of a protein is determined by its amino acid sequence[36,37]. Our discovery that species of the family Neritidae

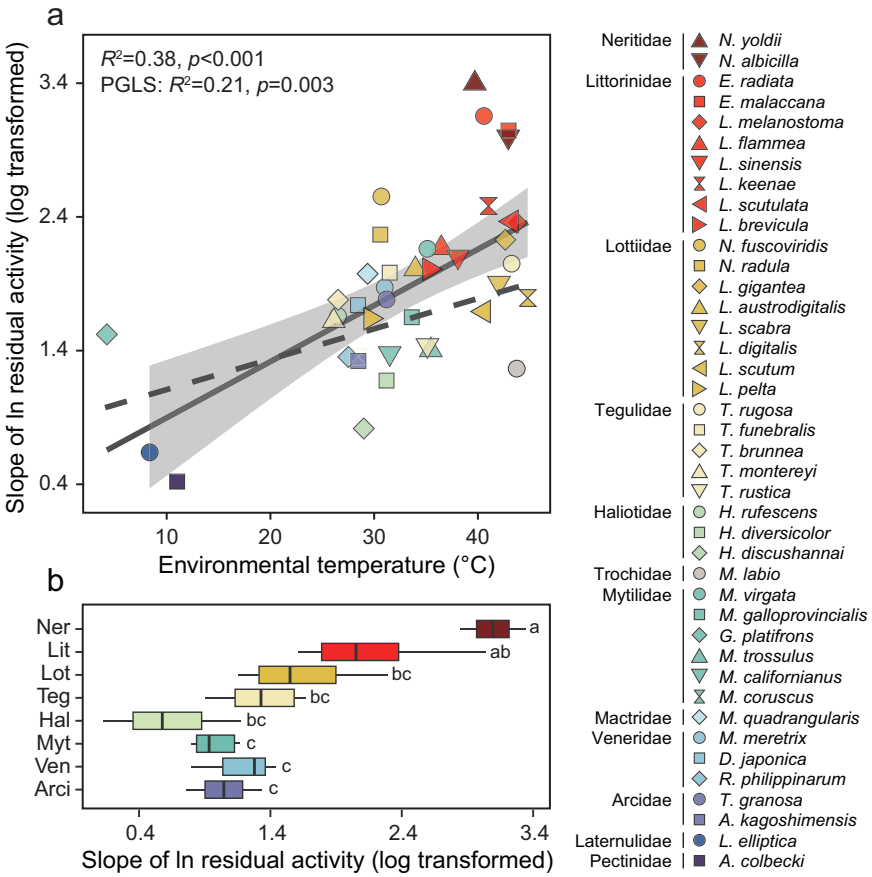


**Fig. 3 | Relationship between the environmental temperature and the thermal stability of cMDH orthologs from the forty-one marine mollusks.** **a** Each point represents the maximal environmental temperature from each species across the global distributions shown in Fig. 1. The shaded zone indicates the 95% confidence interval range. The dashed line represented the PGLS model regression of the data. The solid line represented the linear regression of the data without PGLS model and the association was analyzed using Pearson's correlations test. **b** The ranges of the thermal stability (slope of ln residual activity) of cMDH orthologs from the marine mollusks of the eight family (numbers of species ≥2). Different letters next to the bars indicate significant differences ($P < 0.05$). Data were log-transformed (base 10 logarithm) before the analysis using log-modulus transformation.

that generally occur in the cooler middle intertidal zone, have greater thermal structural stabilities of cMDHs than those of the family Littorinidae that occur in the warmer middle to the high intertidal zone seems consistent with this model of protein evolution. Due to the complexity and variability of intertidal ecosystems and species distributions, it is limited to compare habitat temperature differences based on those data. For example, the two species in Neritidae, *N. albicilla* and *N. yoldii*, are distributed in the middle intertidal zone in tropical and subtropical regions. The high temperature for snails in the tropical middle intertidal zone was lower than that in the tropical high intertidal zone but higher than the temperate high intertidal zone where some Littorinidae snails occur. In other words, at the same latitude, the thermal stress that the middle intertidal Neritidae snails face is lower than that of the high intertidal Littorinidae snail. It is a point we need to focus on in future analyses. Some mutations derived from inferred ancestors can increase the stability of a protein[38–40]. Interestingly, those mutant types can exist under mild conditions that are a little different from those found today. Thus, we hypothesize that the superb thermal adaptation of the cMDH from the family Neritidae may have originated from its ancestor, which lived in a high-temperature environment.

The thermostability of ancestral enzymes would then have been lost gradually through neutral drift in the diversification of the extant enzymes[34]. In our study, the thermal adaptation of cMDH orthologs doesn't absolutely match the intertidal vertical distributions of species and changes as the branches of phylogenetic tree become more distant, suggesting that this ancient thermostability in cMDH orthologs of the families Neritidae that usually inhabit relatively thermally benign mid-intertidal zone may not have been completely lost following the change of environmental temperature. For intertidal animals, the contribution of environmental temperature to thermal adaptation could be not always neutral, because the thermal stress can be extreme in rocky intertidal habitats[41]. Analyzing the phylogenetic relationship of 41 species of marine mollusks could provide insight for interpreting the effect of ancestral genetics on the evolution of thermal tolerances. Results highlight that heat tolerance is highly conserved in the phylogeny, especially in families Neritidae and Littorinidae (Fig. 1), in agreement with studies on the HCTs of gastropods[18], and the upper lethal temperatures (ULTs) of terrestrial ectotherms[19,42,43]. This trend is probably due to conserved characteristics in deep phylogenetic history. The average ages of genera *Littoraria*, *Littorina*, and *Echinolittorina* are about 44−56 million years ago (Ma)[44]. This period is referred to as the Paleocene-Eocene Thermal Maximum (PETM), at which SST rose by 5 °C in the tropics and as much as 9 °C at high latitudes[45]. The average age of genus *Nerita* is reported to be 68.18 Ma[46], coincident with the late Maastrichtian warming event (LMWE), characterized by a global temperature increase of ~2.5–5 °C[47]. These extreme heat events may have contributed to their common ancestor's high heat tolerance. Therefore, the thermal adaptation of cMDH orthologs has probably been from an ancient ancestor. The underlying genetic adaptations due to common ancestry play a crucial role in the evolution of protein thermal tolerances of marine mollusks. The shaping of heat tolerance by thermal history may be more potent and long-lasting than recent or current temperature adaptation.

Compared with the pattern of global structural flexibility of cMDH, a phylogenetically related trend was weaker in the "mobile regions" (MRs, residues 90–105 in MR1 and residues 230–245 in MR2) of cMDH orthologs (Table 1), which are involved in essential conformational changes during catalysis. More remarkable, however, is the significantly positive relationship between the regional stability in MRs and the global structural stability of cMDH orthologs. This suggests that the structural stability in MRs is mainly driven by temperature adaptation rather than phylogenetic history. Our previous studies have shown that the flexibility of the MRs can be readily influenced by even a single amino acid substitution occurring outside of MRs[7,48]; that is, the stability of these flexible regions can be changed easily through mutations or post-translational modifications to adapt to different temperatures[49]. Thus, although the phylogenetic influences on structural stability of cMDH were observed in the species of families Neritidae and

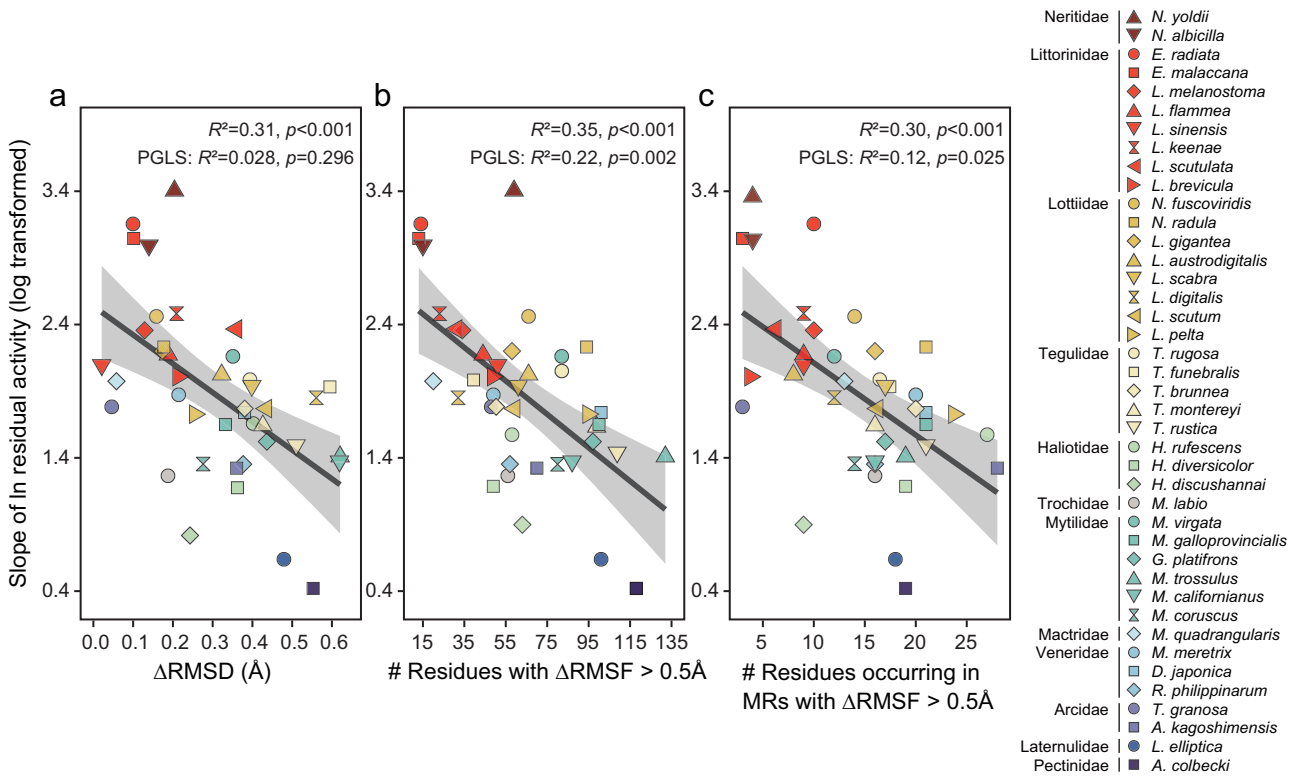


**Fig. 4 | Structural rigidities and flexibilities of the forty-one cMDH orthologs based on molecular dynamics simulations analyses. a** Relationship between the structural rigidity (indicated by the ΔRMSD (the difference of RMSD value between 42 and 15 °C) over the equilibration) with the thermal stability (indicated by the slope of ln residual activity) (log 10 transformed) of the forty-one cMDH orthologs. Relationship between the structural flexibility (indicated by the number of residues with ΔRMSF (the difference of RMSF value between 42 and 15 °C) more than 0.5 Å) **b**, and the structural flexibility in mobile regions (MRs) (indicated by the number of residues 90–105 and 230–245 with ΔRMSF > 0.5 Å) with the thermal stability of the cMDH orthologs (**c**). The shaded zone indicates the 95% confidence interval range. The solid line represented the linear regression of the data without PGLS model and the association was analyzed using Pearson's correlations test.

Littorinidae, there are still flexible regions essential for catalytic conformational changes that are influenced by selection pressure arising from the environmental temperature.

### Evolution and stability of proteins structure

The stability of a protein's structure determines not only the species' temperature adaptation capacity but also its evolutionary capacity. The relationships related to environmental adaptation between compositional peculiarities and sequence biases reflected molecular adaptation on DNA, RNA, and protein levels[50]. For example, in the process of the coevolution of nucleic acids and proteins, thermal stability related demands on the amino acid composition affect the nucleotide content in the second codon position in Archaea[50]. Trade-offs among the structure, dynamics, and function associated with the thermal adaptation strategies of protein molecules help to understand how proteins have evolved in their native environments[51]. The structural stability of proteins at all levels has a non-negligible role in evolution, and the influence of structural stability on the evolution of protein structure is complex. On the one hand, one protein sequence can adopt multiple folded structures (conformations), and this inherent conformational variation has been proposed to be the foundation of evolvability[52,53]. In this case, the increased global stability and reduced conformational flexibility of warm-adapted species may limit the conformational diversity of orthologs and restrict the evolution of protein thermal adaptation[54]. On the other hand, most random mutations (functionally beneficial or not) are destabilized[55]. The larger excess of stability enables a larger number of beneficial but destabilizing mutations to be accommodated while retaining protein fitness[53]. In this case, the stability will promote the evolution. For many marine mollusks that live in the high intertidal zone, such as the family Littorinidae, the evolutionary rate of cMDH is limited by their highly structural stability, which will exacerbate the threat of global warming to them. However, for the two species in Neritidae in our study, their heat tolerance is quite abundant for the current environmental temperature, so their excessive stability can help them survive in future rising temperatures.

### mRNA stability and phylogenetic traits

mRNA stabilities of cMDH orthologs from differently thermally adapted marine mollusks exhibit phylogenetic patterns similar to those found for the cMDH protein. For example, the cMDH orthologs from Neritidae and Littorinidae, with a common ancestor, had more stable secondary structures of mRNA than other snails in our study. Recent experimental evidence on the evolutionary conservation of mRNA structures suggested an inherent trade-off, e.g., the trade-off between secondary structure and tRNA-concentration in *Saccharomyces cerevisiae* and *Escherichia coli*, under selective pressures acting at the RNA level[56–60]. In both prokaryotes and eukaryotes, the mRNA stability indicated by $\Delta G_{fold}$ correlates with the mRNA length and the evolutionary rate of synonymous positions[59]. Our previous study showed that the contents of G + C were not only significantly positively correlated with $\Delta G_{fold}$, but also correlated with the adaptation temperatures of species[8]. Influenced by the ionic strength[61] as well as the proteins and other molecules that stabilize the RNA[62,63], a higher proportion of G:C pairs increases the thermodynamic stability of RNA[64]. The mRNA of cMDH in warm-adapted species possesses more G:C pairs and vice versa in cold-adapted species[8]. Therefore, the contents of G + C and $\Delta G_{fold}$ are reliable tools for identifying the structural stability and thermal adaptation of mRNAs. RNA structure can influence each step of protein expression and RNA stability can play a number of important roles under stress conditions[65]. In the present study, the free energy of formation ($\Delta G_{fold}$) and the G + C content acted as an indicator for evaluating the stability of mRNA secondary structures; the absolute value of $\Delta G_{fold}$ was inversely related to the thermal resistance of the protein orthologs,

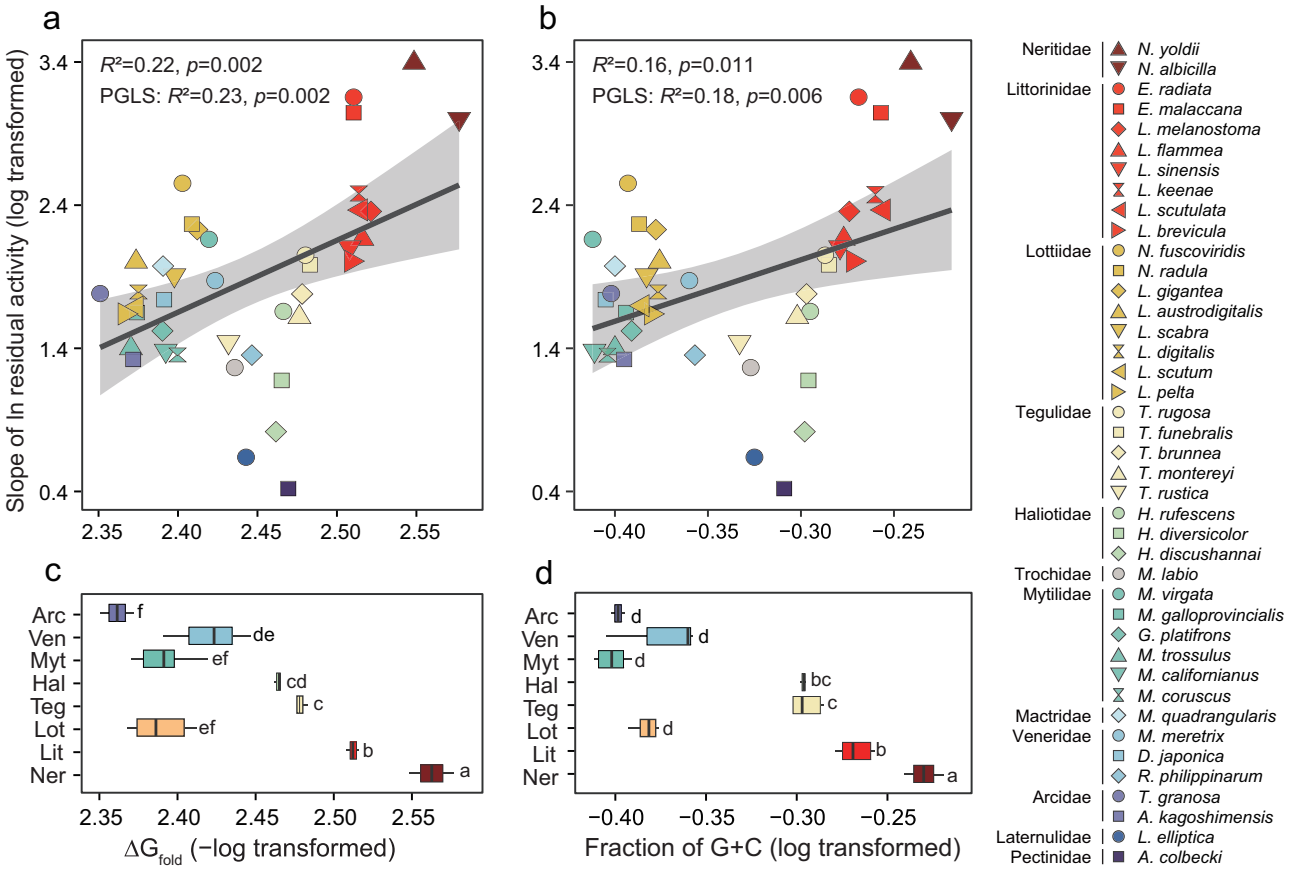


**Fig. 5 | Structural stabilities of the cMDH mRNAs from forty-one marine mollusks.** Relationship between the change in free energy of formation ($\Delta G_{fold}$) (log 10 transformed) of each secondary structure ensemble of cMDH mRNAs (**a**), and the fraction of G + C (log 10 transformed) (**b**) with the thermal stability (indicated by the slope of ln residual activity) (log 10 transformed) of the encoded proteins. The shaded zone indicated the 95% confidence interval range. The corresponding range of the $\Delta G_{fold}$ (−log 10 transformed) (**c**) and fraction of G + C (log 10 transformed) (**d**) of the cMDH orthologs from marine mollusks in the eight families (numbers of species ≥2). Different letters next to the bars indicate significant differences ($P < 0.05$). The solid line represented the regression of the data without PGLS model.

consistent pattern was found from the G + C content. The highly structured mRNAs may retain their structural stability under temperature shifts, mutations, and changes in UTRs[66]. Thus, the appropriate structural stability of mRNA can ensure the stable expression and evolution of cMDH in different environmental temperatures. Park et al.[23] found that amino acid substitution rate is negatively correlated with mRNA folding strength, with or without the control of expression level, demonstrating a major role of natural selection at the mRNA level in constraining protein evolution. In addition, the folding specificity of mRNAs is lower than that of ncRNAs and exhibits moderate evolutionary conservation[67]. Therefore, mRNA folding plays a major role in the constraining functional evolution of proteins.

## Conclusion

In summary, protein stability is not only a consequence of environmental selection driven by habitat (body) temperature but also a product of neutral evolution. The upper limit of protein stability has strong phylogenetic conservatism. Our results emphasize the importance of evolutionary history in shaping biological thermal tolerance, a conclusion that has important implications for organisms' ability to respond to global warming. In addition, the "excessive stability" has a higher tolerance for unstable functional mutations and increasing temperatures, which is beneficial for survival and evolution in the context of a warming climate.

## Materials and methods

### Specimen collection

Specimens of *Dosinia japonicum*, *Meretrix meretrix*, *Mactra quadrangularis*, and *Anadara kagoshimensis* were collected from Panjin, China (40.90 °N, 121.85 °E), in July 2021. *Ruditapes philippinarum*, *Tegillarca granosa*, *Mytilisepta virgata*, *Tegula rustica*, and *Monodonta labio* were collected from Zhangzhou, China (23.65 °N, 117.49 °E), in May to August 2021. *Littorina brevicula* was collected from Qingdao, China (36.06 °N, 120.33 °E), from August to September 2021. *Littoraria sinensis* was collected in Qidong, China (32.11 °N, 121.59 °E), in January 2021. *Littoraria flammea* was collected in Nantong, China (32.11 °N, 121.40 °E), in October 2021. *Littoraria melanostoma* was collected in Wenzhou, China (27.86 °N, 121.14 °E), in November 2020. *Mytilus coruscus* was collected from Dongji Island, China (28.72 °N, 121.93 °E) in November 2021. All specimens were transported alive to the laboratory within 24 h and subjected to at least one week of indoor acclimation (temperature: ~16 °C, pH: ~8, and salinity: ~30 psu). After acclimation, the adductor muscles of individuals were dissected and stored at −80 °C for further laboratory studies. The deep-sea mussel, *G. platifrons* was collected from a methane seep (22.12 °N, 119.29 °E, 1130 m deep) in the South China Sea in May 2018. The mussels were frozen in liquid nitrogen and stored at −80 °C until used for further laboratory studies. The species used in the present study is invertebrate, and all specimens are not protected animal, and the sampling site is not in reserve. No ethical approval or permit was required for collecting these species.

### Present environmental temperature

The environmental temperature data was calculated by the methods described in Ma et al.[68]. The monthly global climate data at ~4 km (1/24th degree) spatial resolution from 2000 to 2014 were obtained at TerraClimate. The Tide Model Driver (TMD) in MATLAB R2022a (MathWorks, Natick, Massachusetts) was applied to predict hourly tidal height data for the global

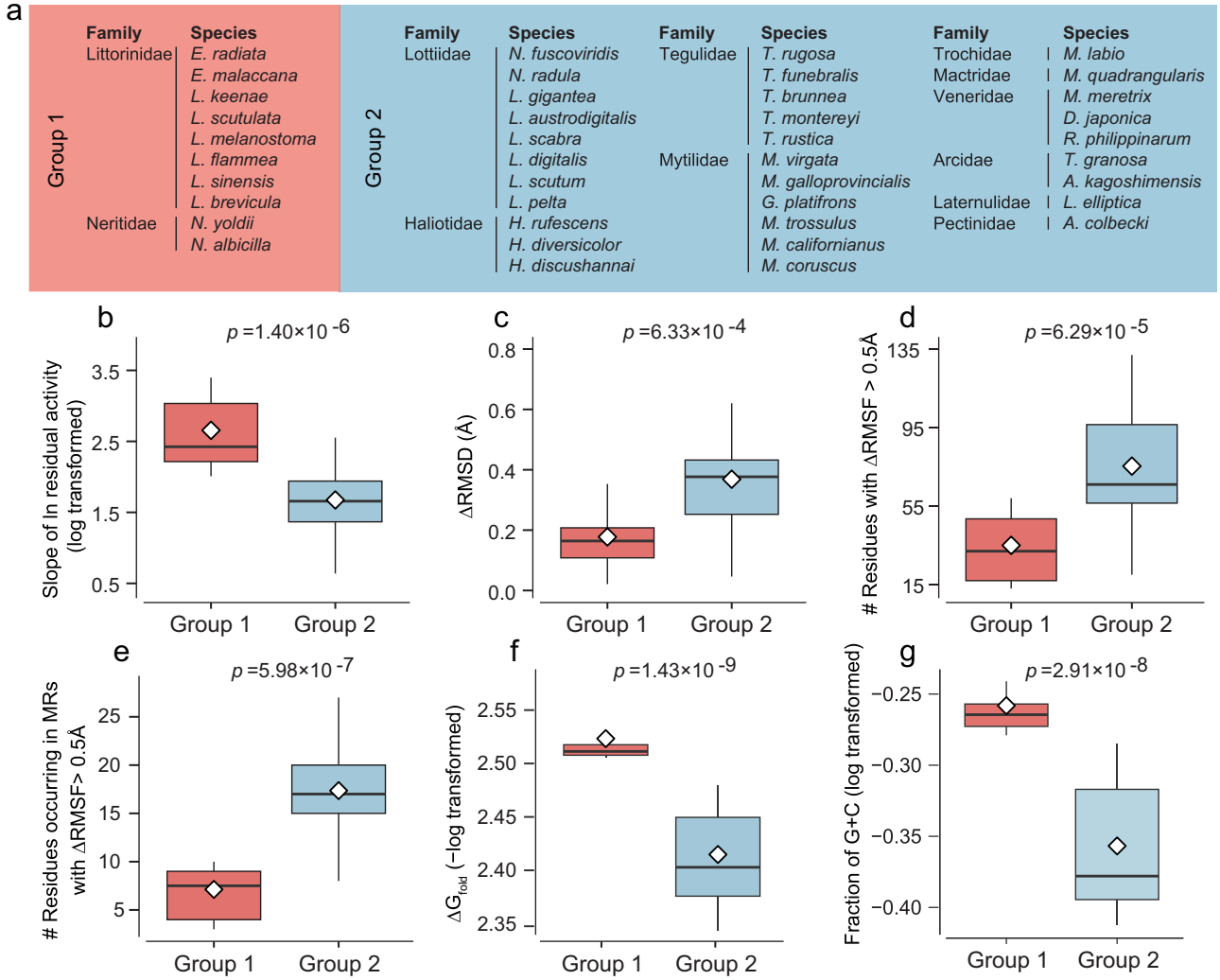


**Fig. 6 | Thermal stabilities, structural rigidities, and flexibilities of the cMDH orthologs, and structural stabilities of the cMDH mRNAs from forty-one marine mollusks. a** Two clusters of forty-one marine mollusks in association analysis using two-step cluster analysis based on the slope of ln residual activity, the ΔRMSD, $\Delta G_{fold}$, and fraction of G + C. **b** The thermal stabilities of the cMDH orthologs indicated by the slope of ln residual activity. The structural rigidities and flexibilities of the cMDH orthologs indicated by the ΔRMSD (**c**), the number of residues with ΔRMSF > 0.5 Å (**d**), and the number of residues occurring in MRs with ΔRMSF > 0.5 Å (**e**), respectively. The structural stabilities of the cMDH mRNAs are indicated by the $\Delta G_{fold}$ (**f**) and fraction of G + C (**g**). All indexes showed significant differences ($P < 0.001$).

intertidal zone. We calculated the hourly body temperature of the snails using a heat budget model (HBM), an improved version of the simple snail's HBM, initially derived from mussels, incorporating more comprehensive biological morphological characteristics and supplementary calculation procedures[20,69,70]. The mean values of estimated body temperatures of mollusks living in the splash zone, high intertidal, and middle intertidal were calculated, respectively. The 95th percentile of maximal body temperatures of mollusks that live in splash zone, high intertidal, and mid intertidal were extracted to represent the corresponding environmental temperatures, respectively.

SSTs every 3 h from 2000 to 2014, reported by the Earth System Grid Federation with 250 km nominal resolution, were downloaded from CMIP6. The 95th percentile of maximal SST was extracted as the environmental temperature of low intertidal species. Annual sea temperatures on a 0.25° grid from 2007 to 2018 were obtained at WOA18 (World Ocean Atlas 2018) dataset from the National Centers for Environmental Information (https://www.nodc.noaa.gov/cgi-bin/OC5/woa18/woa18.pl/). The maximal water temperature at a depth of 1150 m was chosen to represent the environmental temperature of deep-sea mussel (*G. platifrons*).

### Phylogenetic tree

The backbone of phylogeny among 41 selected molluscan species was established based on existing studies[44,71–75]. Further, the Cytochrome c oxidase subunit I gene sequences (Supplementary Table 5) were aligned with Mafft software[76], followed by the construction of ML trees by FastTree v2.1.11 with generalized time-reversible model (-gtr parameter)[77], to verify or determine the phylogenetic relationships within genera.

### Phylogenetic signal and PGLS analysis

The mitochondrial cytochrome oxidase subunit I (COI) genes of the 41 species were used for phylogenetic signal estimation and phylogenetic generalized least squares (PGLS) analyses (Supplementary Table 5). A tailed mussel, *Lingula anatine*, was chosen as the outgroup for the comparisons. A phylogenetic tree was constructed using Maximum-likelihood (ML) and Bayesian inference methods. The ML tree was generated using MEGA11 under the General Time Reversible (TR) model by using a discrete Gamma distribution (+G) of substitution with 1000 replicates[78].

The phylogenetic signal indicates the extent to which closely related species tend to resemble each other. We computed the Blomberg's $K$[25] and Moran's $I$[26] of all stability indexes using function *phylosignal* in R package

*phylosignal*[79]. $K = 0$ indicates no phylogenetic signal, and $K = 1$ suggests that the trait distribution perfectly conforms to Brownian Motion (BM)[25]. Moran's $I$ varies from −1.0 to +1.0, a significant positive value indicates high similarity between closely related species, while a significant negative value denotes that related species are dissimilar[26]. PGLS model is used to establish the nature of the evolutionary association between two or more biological traits, that is the evidence that traits are associated over evolutionary time[31]. The analyses of PGLS were conducted according to the methods described previously, using the R package tools *ape* and *caper*[80,81], to account for possible phylogenetic effects on the observations[82].

### Determination of thermal stabilities of cMDH

The thermal stabilities of cMDH orthologs were determined by the methods described in Dong and Somero[48] and Liao et al.[32]. Non-denaturing polyacrylamide gel electrophoresis (Native-PAGE) was used to determine the heating temperature needed to eliminate the more thermally labile mitochondrial isoform of MDH (mMDH). Enzyme preparation involved ammonium sulfate precipitation of heat-treated homogenates (heating removed the thermally labile mMDH) to isolate a cMDH-rich protein fraction. After overnight dialysis, enzymes were diluted to equivalent activity and incubated in a buffer containing 200 mmol $l^{-1}$ imidazole-HCl, 150 μmol $l^{-1}$ NADH and 200 μmol $l^{-1}$ OAA at 42.5 °C for different times ($t$ = 0, 5, 10, 15, 20, 25, 30, 45, and 60 min)[32]. Residual activities were determined at 25 °C using a UV-1900 spectrophotometer (Shimadzu, Kyoto, Japan) with a temperature-controlled cell attached to a water bath (Tianheng, Ningbo, China). Residual activity was defined as the ratio between the mean activity at time t and the mean activity at time 0. Residual activity at different times was ln-transformed and then fitted to time; the slope of residual activity obtained were log-modulus transformed (base 10 logarithm) before the analysis to indicate the thermal stability of cMDH orthologs, i.e., higher values represent greater stability. Previous studies have demonstrated that the thermal stability of cMDH orthologs, as indicated by the slope of ln residual activity (log transformed), is a valid and reliable criterion for comparing adaptation temperatures[3,7,8,33].

### Sequencing of cMDH cDNA

The cMDH cDNA sequences and the thermal residual activity for 25 cMDH orthologs of marine mollusks were obtained from previous studies (Supplementary Table 5)[7,32,33,48,83,84]. The cMDH cDNA sequences of orthologs that had not been sequenced previously were sequenced as described by Dong and Somero[48]. Total RNA was purified from adductor muscle using Trizol reagent (Invitrogen, Carlsbad, CA, USA). The pre-designed primers (MDF1 and MDR1) were used to amplify partial sequences. The full-length cDNAs of cMDH were obtained using the rapid amplification of cDNA ends (RACE) method. The targeted fragment was assembled and introduced into a plasmid which was then transformed into *E. coli* strain DH5α (TaKaRa, Dalian, China). Finally, the individual plasmids were sequenced using Sanger sequencing (Sangon Biotech, Shanghai, China). The sequences of primers used in this study are given in Supplementary Table 6.

### Molecular dynamic simulation of cMDH

MDS is used to evaluate global flexibility of structure (RMSD: the root means square deviation) and localized flexibility of individual amino acid residues (RMSF: the root mean square fluctuation). Using the sequence data of cMDH cDNAs, 3D models of the enzyme were constructed by the I-TASSER server[85]. The computed 3D structures constructed above were used as the starting models of the simulations. Simulations were performed by using NAMD (Version 2.9) with the CHARMM36 force field[86–89]. Each system was assigned for 20 ns at 15 and 42 °C in triplicate for all simulations. 20 ns was selected as a suitable and economical timeframe for the MDS of molluscan cMDH according to previous study[33]. Trajectories of the structures were collected every 0.002 ns. Every 0.002 ns of the actual frame was stored during the simulation. The system set-up was provided in Supplementary Table 7. For more details see our previous study[7].

The VMD program was used to visualize and analyze the simulation trajectories[90]. The RMSD of backbone atom positions and the RMSF for individual residues in all models were calculated and compared. They are defined as: $\mathrm{RMSD} = \sqrt{\frac{1}{N}\sum_{i=1}^{N}(r_i - r_o)^2}$ and $\mathrm{RMSF} = \sqrt{\frac{1}{N}\sum_{i=1}^{N}(r_i - r)^2}$, where $r_i$ represents the position at time $i$, and $r_0$ represents the reference value, $r$ represents the average value of the RMSF, and $N$ represents the number of atoms. The stabilized structure (10−15 ns) (Supplementary Fig. 3) was taken from the system's trajectory to determine the movements of the protein backbone and individual residue atoms. The averaged equilibrium RMSD of backbone atom positions and averaged equilibrium RMSF for individual residues were calculated and compared. The differences between the values obtained at 15 and 42 °C for RMSD (ΔRMSD: $\Delta\mathrm{RMSD} = \mathrm{RMSD}_{42°C} - \mathrm{RMSD}_{15°C}$) and RMSF (ΔRMSF: $\Delta\mathrm{RMSF} = \mathrm{RMSF}_{42°C} - \mathrm{RMSF}_{15°C}$) were calculated to estimate protein rigidity and flexibility.

### Secondary structure prediction of cMDH mRNA

Secondary structure predictions from individual coding sequences (CDSs) of cMDH mRNAs were conducted using the Vienna RNA package (v. 2.4.17)[91]. The free energy change that occurs during the formation of mRNA secondary structure ($\Delta G_{fold}$) was calculated using the efn2 algorithm at a temperature of 37 °C for all cMDH mRNA orthologs[92]. The original value of $\Delta G_{fold}$ is negative, we multiplied this value by −1 and then log-transformed (base 10 logarithm)[8]. The absolute values of log-transformed $\Delta G_{fold}$ were used to indicate the stability of cMDH mRNA. G + C content was counted based on the results of secondary structure predictions. Those data also were log transformed (base 10 logarithm) before the analysis. Above two indexes ($\Delta G_{fold}$ and G + C content) were used to quantize the structural stabilities of the cMDH mRNAs.

### Expression and purification of recombinant enzymes

Four representative species (*Echinolittorina malaccana*, *E. radiata*, *L. keenae* and *M. galloprovincialis*) were selected to construct recombinant proteins. cMDHs cDNAs were amplified by PCR using pairs of primers with restriction sites for EcoRI and HindIII (Supplementary Table 6). PCR products were purified and ligated to pMD19 (TaKaRa, Dalian, China) using T4 DNA ligase (TaKaRa, Dalian, China) to generate the recombinant plasmids. The E. coli DH5α (TaKaRa, Dalian, China) was used for initial cloning of pMD19-cMDH. All of the pMD19-cMDHs were purified and digested by EcoRI and HindIII (Yeasen, Shanghai, China) and then cloned into vectors pET32a(+) that digested by the same restriction enzyme above. Those pET32a(+) recombinant vectors were transformed into expression hosts, *E. coli* BL21(DE3) chemically competent cells (Weidi), and plated on Luria-Bertani (LB) agar medium containing ampicillin (100 μg/mL) at 37 °C overnight. Plasmids were purified from individual colonies using an extraction kit (TaKaRa, Dalian, China). The sequences of target cMDHs in plasmids were verified by DNA sequencing.

Correctly sequenced individual colonies were inoculated in 3 L of LB/ampicillin broth and grown to log phase with vigorous shaking (180 rpm) at 37 °C for ~6 h. Isopropyl-β-D-thiogalactopyranoside (IPTG) was added to a final concentration of 1 mmol/L for expressions of target fusion proteins. The incubation period continued for another 6 h at 30 °C with shaking at 220 rpm. After inductions, the bacteria cells were pelleted at 8000 rpm for 10 min. The expressed protein was purified using an Ni-NTA Sepharose Resin (Sangon Biotech, Shanghai, China) at 4 °C. The pellet was resuspended in 10 mL lysis buffer (50 mmol/L potassium phosphate, pH 6.8). Extraction was performed by an ultrasonic cell disruptor (Scientz, Zhejiang, China) with 30% amplitude kept cold by an ice water mixture (an extraction cycle with 10 s disruption and 10 s rest, in total 10 min). The cell suspension was then centrifuged at 9500 rpm and 4 °C for 90 min. The supernatant was mixed with 5-mL Ni-NTA agarose resin to incubate at 4 °C for 30 min, which allowed the resin to fully bind the poly His-tag attached to the N-terminus of the recombinant cMDH and enabled rapid purification. And then the resin was washed (20 mL of 50 mmol/L potassium phosphate, pH

7.4, 300 mmol/L NaCl, 10 mM imidazole), the purified cMDH was eluted with 10 mL wash buffer plus 250 mmol/L imidazole. The purified protein passed over a chromatography column (Superose™ 6 Increase SEC, Cytiva, Shanghai, China) with potassium phosphate buffer (50 mmol/L, pH 6.8) to further purify the target protein. The qualities of purified recombinant proteins were analyzed on SDS-PAGE gel electrophoresis.

### Determination of melting temperature ($T_m$) of cMDH

CD spectra were determined on a Jasco J-1500 spectropolarimeter (Jasco, Japan) at wavelengths from 190 to 250 nm to ensure the structural integrity of the protein prior to analysis. The purified protein in 50 mM phosphate buffer (pH 6.8) was measured with a 1 mm cell in the far-UV region. At wavelength of 222 nm, variable temperature spectra were measured from 30 to 70 °C, and were intercepted for the proteolysis temperature interval and Tm values were calculated using software SpectraManager.

### Statistics and reproducibility

All statistical analyses were done in R (v. 3.5.3). The association was analyzed using Pearson's correlation test. Differences between families (numbers of species ≥2) were analyzed using a one-way variance analysis followed by least significance difference ($P < 0.05$). We set up three replicates for the determination of cMDH thermal stability. The MDS simulations were set up with 5−10 replications per structure, and finally three structural trajectories that remained stable at 10−15 ns were selected for subsequent calculations.

### Reporting summary

Further information on research design is available in the Nature Portfolio Reporting Summary linked to this article.

## Data availability

The cMDH mRNA sequences reported in this paper have been deposited in the GenBank database (accession nos. PQ594415, PQ594416, PQ594417, PQ594418, PQ594419, PQ594420, PQ594421, PQ594422, PQ594423, PQ594424, PQ594425, PQ594426, PQ594427, PQ594428, and PQ609679). The environmental temperature and distribution of the species studied have been deposited in the Supplementary data 1 and 2. Data used to create the Figures have been deposited in the Supplementary data 3. The simulation input files for the MDS have been deposited in figshare[93]; all the trajectory files for the MDS can be obtained by contacting the corresponding author upon reasonable request. Other data used are available in the main text or the supplementary materials.

## Code availability

Custom code for performing simulation and analysis is available from the cited references in the paper.

Received: 20 June 2024; Accepted: 4 March 2025;
Published online: 20 March 2025

## References

1. Addo-Bediako, A., Chown, S. L. & Gaston, K. J. Thermal tolerance, climatic variability and latitude. *P. Roy. Soc. B Biol. Sci.* **267**, 739–745 (2000).
2. Garcia-Robledo, C., Kuprewicz, E. K., Staines, C. L., Erwin, T. L. & Kress, W. J. Limited tolerance by insects to high temperatures across tropical elevational gradients and the implications of global warming for extinction. *Proc. Natl. Acad. Sci. USA* **113**, 680–685 (2016).
3. Somero, G. N., Lockwood, B. L. & Tomanek, L. *Biochemical Adaptation: Response to Environmental Challenges from Life's Origins to the Anthropocene* (Sinauer Associates, 2017).
4. Dong, Y. W. et al. Biological traits, geographic distributions, and species conservation in aquatic ecosystems. *Divers. Distrib.* **28**, 1516–1523 (2022).
5. Dong, Y. W. Roles of multi-level temperature-adaptive responses and microhabitat variation in establishing distributions of intertidal species. *J. Exp. Biol.* **226**, jeb246544 (2023).
6. Fields, P. A. Review: Protein function at thermal extremes: balancing stability and flexibility. *Comp. Biochem. Phys. A.* **129**, 417–431 (2001).
7. Dong, Y. W., Liao, M. L., Meng, X. L. & Somero, G. N. Structural flexibility and protein adaptation to temperature: molecular dynamics analysis of malate dehydrogenases of marine molluscs. *Proc. Natl. Acad. Sci. USA* **115**, 1274–1279 (2018).
8. Liao, M. L., Somero, G. N. & Dong, Y. W. Thermal adaptation of mRNA secondary structure: stability versus lability. *Proc. Natl. Acad. Sci. USA* **118**, e2113324118 (2021).
9. Pinney, M. M. et al. Parallel molecular mechanisms for enzyme temperature adaptation. *Science* **371**, 1010 (2021).
10. Kellermann, V., Hoffmann, A. A., Overgaard, J., Loeschcke, V. & Sgrò, C. M. Plasticity for desiccation tolerance across *Drosophila* species is affected by phylogeny and climate in complex ways. *P. Roy. Soc. B Biol. Sci.* **285**, 20180048 (2018).
11. Dahlke, F. T., Wohlrab, S., Butzin, M. & Pörtner, H.-O. Thermal bottlenecks in the life cycle define climate vulnerability of fish. *Science* **369**, 65–70 (2020).
12. Anderson, S. I., Barton, A. D., Clayton, S., Dutkiewicz, S. & Rynearson, T. A. Marine phytoplankton functional types exhibit diverse responses to thermal change. *Nat. Commun.* **12**, 6413 (2021).
13. Hou, Q., Rooman, M. & Pucci, F. Enzyme stability-activity trade-off: new insights from protein stability weaknesses and evolutionary conservation. *J. Chem. Theory Comput.* **19**, 3664–3671 (2023).
14. Ribeiro, A. J. M., Riziotis, I. G., Borkakoti, N. & Thornton, J. M. Enzyme function and evolution through the lens of bioinformatics. *Biochem. J.* **480**, 1845–1863 (2023).
15. Chown, S. L. Macrophysiology for decision-making. *J. Zool.* **319**, 1–22 (2023).
16. Araújo, M. B. et al. Heat freezes niche evolution. *Ecol. Lett.* **16**, 1206–1219 (2013).
17. Smith, E. G. et al. Signatures of selection underpinning rapid coral adaptation to the world's warmest reefs. *Sci. Adv.* **8**, eabl7287 (2022).
18. McMahon, R. F. Acute thermal tolerance in intertidal gastropods relative to latitude, superfamily, zonation and habitat with special reference to the Littorinoidea. *J. Shellfish Res.* **20**, 459–467 (2001).
19. Kellermann, V. et al. Upper thermal limits of *Drosophila* are linked to species distributions and strongly constrained phylogenetically. *Proc. Natl. Acad. Sci. USA* **109**, 16228–16233 (2021).
20. Arcus, V. L., van der Kamp, M. W., Pudney, C. R. & Mulholland, A. J. Enzyme evolution and the temperature dependence of enzyme catalysis. *Curr. Opin. Struct. Biol.* **65**, 96–101 (2020).
21. Chao, Y. C., Merritt, M., Schaefferkoetter, D. & Evans, T. G. High-throughput quantification of protein structural change reveals potential mechanisms of temperature adaptation in Mytilus mussels. *BMC Evol. Biol.* **20**, 28 (2020).
22. Marasco, R. et al. Enzyme adaptation to habitat thermal legacy shapes the thermal plasticity of marine microbiomes. *Nat. Commun.* **14**, 1045 (2023).
23. Park, C., Chen, X., Yang, J. R. & Zhang, J. Differential requirements for mRNA folding partially explain why highly expressed proteins evolve slowly. *Proc. Natl. Acad. Sci. USA* **110**, E678–E686 (2013).
24. Münkemüller, T. et al. How to measure and test phylogenetic signal. *Methods Ecol. Evol.* **3**, 743–756 (2012).
25. Blomberg, S. P., Garland, T. Jr & Ives, A. R. Testing for phylogenetic signal in comparative data: behavioral traits are more labile. *Evolution* **57**, 717–745 (2003).
26. Gittleman, J. L. & Kot, M. Adaptation: statistics and a null model for estimating phylogenetic effects. *Syst. Biol.* **39**, 227–241 (1990).
27. Ávila-Lovera, E., Winter, K. & Goldsmith, G. R. Evidence for phylogenetic signal and correlated evolution in plant-water relation traits. *New Phytol.* **237**, 392–407 (2022).
28. Faria, S. C., Provete, D. B., Thurman, C. L. & McNamara, J. C. Phylogenetic patterns and the adaptive evolution of osmoregulation in fiddler crabs (Brachyura, *Uca*). *Plos ONE***12**, e0171870 (2017).

29. Liu, H. et al. Strong phylogenetic signals and phylogenetic niche conservatism in ecophysiological traits across divergent lineages of Magnoliaceae. *Sci. Rep.* **5**, 12246 (2015).
30. Ma, Z. et al. Evolutionary history resolves global organization of root functional traits. *Nature* **555**, 94–97 (2018).
31. Symonds, M. R. E. & Blomberg, S. P. A primer on phylogenetic generalised least squares. In (ed Garamszegi, L. Z.) *Modern Phylogenetic Comparative Methods and Their Application in Evolutionary Biology: Concepts and Practice* (Springer, 2014).
32. Liao, M. L. et al. Heat-resistant cytosolic malate dehydrogenases (cMDHs) of thermophilic intertidal snails (genus *Echinolittorina*): protein underpinnings of tolerance to body temperatures reaching 55°. *C. J. Exp. Biol.* **220**, 2066–2075 (2017).
33. Liao, M. L., Somero, G. N. & Dong, Y. W. Comparing mutagenesis and simulations as tools for identifying functionally important sequence changes for protein thermal adaptation. *Proc. Natl Acad. Sci. USA* **116**, 679–688 (2019).
34. Nguyen, V. et al. Evolutionary drivers of thermoadaptation in enzyme catalysis. *Science* **355**, 289–294 (2017).
35. Gumulya, Y. et al. Engineering highly functional thermostable proteins using ancestral sequence reconstruction. *Nat. Catal.* **1**, 878–888 (2018).
36. Anfinsen, C. B. Principles that govern the folding of protein chains. *Science* **181**, 223–230 (1973).
37. Martin, O. A. & Vila, J. A. The marginal stability of proteins: how the jiggling and wiggling of atoms is connected to neutral evolution. *J. Mol. Evol.* **88**, 424–426 (2020).
38. Watanabe, K., Ohkuri, T., Yokobori, S.-I. & Yamagishi, A. Designing thermostable proteins: ancestral mutants of 3-isopropylmalate dehydrogenase designed by using a phylogenetic tree. *J. Mol. Biol.* **355**, 664–674 (2006).
39. Yamashiro, K., Yokobori, S.-I., Koikeda, S. & Yamagishi, A. Improvement of *Bacillus circulans* β-amylase activity attained using the ancestral mutation method. *Protein Eng. Des. Sel.* **23**, 519–528 (2010).
40. Romero-Romero, M. L. et al. Selection for protein kinetic stability connects denaturation temperatures to organismal temperatures and provides clues to archaean life. *PloS ONE***11**, e0156657 (2016).
41. Helmuth, B. et al. Climate change and latitudinal patterns of intertidal thermal stress. *Science* **298**, 1015–1017 (2002).
42. Clusella-Trullas, S., Blackburn, T. M. & Chown, S. L. Climatic predictors of temperature performance curve parameters in ectotherms imply complex responses to climate change. *Am. Nat.* **177**, 738–751 (2011).
43. Grigg, J. W. & Buckley, L. B. Conservatism of lizard thermal tolerances and body temperatures across evolutionary history and geography. *Biol. Lett.* **9**, 1–4 (2013).
44. Reid, D. G., Dyal, P. & Williams, S. T. A global molecular phylogeny of 147 periwinkle species (Gastropoda, Littorininae). *Zool. Scr.* **41**, 125–136 (2012).
45. Zachos, J. C. et al. Rapid acidification of the ocean during the Paleocene-Eocene thermal maximum. *Science* **308**, 1611–1615 (2005).
46. Feng, J. T. et al. Characterization of four mitochondrial genomes of family Neritidae (Gastropoda: Neritimorpha) and insight into its phylogenetic relationships. *Sci. Rep.* **11**, 11748 (2021).
47. Barnet, J. S. K. et al. A new high-resolution chronology for the late Maastrichtian warming event: Establishing robust temporal links with the onset of Deccan volcanism. *Geology* **46**, 147–150 (2017).
48. Dong, Y. W. & Somero, G. N. Temperature adaptation of cytosolic malate dehydrogenases of limpets (genus *Lottia*): differences in stability and function due to minor changes in sequence correlate with biogeographic and vertical distributions. *J. Exp. Biol.* **212**, 169–177 (2009).
49. Lee, J. M., Hammaren, H. M., Savitski, M. M. & Baek, S. H. Control of protein stability by post-translational modifications. *Nat. Commun.* **14**, 201 (2023).
50. Goncearenco, A., Ma, B. G. & Berezovsky, I. N. Molecular mechanisms of adaptation emerging from the physics and evolution of nucleic acids and proteins. *Nucleic Acids Res.* **42**, 2879–2892 (2014).
51. Fusco, G., Bemporad, F., Chiti, F., Dobson, C. M. & De Simone, A. The role of structural dynamics in the thermal adaptation of hyperthermophilic enzymes. *Front. Mol. Biosci.* **9**, 981312 (2022).
52. James, L. C. & Tawfik, D. S. Conformational diversity and protein evolution – a 60-year-old hypothesis revisited. *Trends Biochem. Sci.* **28**, 361–368 (2003).
53. Tokuriki, N. & Tawfik, D. S. Protein dynamism and evolvability. *Science* **324**, 203–207 (2009).
54. Agozzino, L. & Dill, K. A. Protein evolution speed depends on its stability and abundance and on chaperone concentrations. *Proc. Natl Acad. Sci. USA* **115**, 9092–9097 (2018).
55. Bloom, J. D., Labthavikul, S. T., Otey, C. R. & Arnold, F. H. Protein stability promotes evolvability. *Proc. Natl Acad. Sci. USA* **103**, 5869–5874 (2006).
56. Shabalina, S. A., Ogurtsov, A. Y., Spiridonov, N. A. & Koonin, E. V. Evolution at protein ends: major contribution of alternative transcription initiation and termination to the transcriptome and proteome diversity in mammals. *Nucleic Acids Res.* **42**, 7132–7144 (2014).
57. Gorochowski, T. E., Ignatova, Z., Bovenberg, R. A. L. & Roubos, J. A. Trade-offs between tRNA abundance and mRNA secondary structure support smoothing of translation elongation rate. *Nucleic Acids Res.* **43**, 3022–3032 (2015).
58. Bevilacqua, P. C., Ritchey, L. E., Su, Z. & Assmann, S. M. Genome-wide analysis of RNA secondary structure. *Annu. Rev. Genet.* **50**, 235–266 (2016).
59. Faure, G., Ogurtsov, A. Y., Shabalina, S. A. & Koonin, E. V. Role of mRNA structure in the control of protein folding. *Nucleic Acids Res.* **44**, 10898–10911 (2016).
60. Rivas, E. Evolutionary conservation of RNA sequence and structure. *WIREs RNA* **12**, e1649 (2021).
61. Nakano, S. Nucleic acid duplex stability: influence of base composition on cation effects. *Nucleic Acids Res.* **27**, 2957–2965 (1999).
62. Draper, D. E., Grilley, D. & Soto, A. M. Ions and RNA Folding. *Annu. Rev. Biophys.* **34**, 221–243 (2005).
63. Fischer, N. M., Polêto, M. D., Steuer, J. & van der Spoel, D. Influence of Na+ and Mg2+ ions on rna structures studied with molecular dynamics simulations. *Nucleic Acids Res.* **46**, 4872–4882 (2018).
64. Kornienko, I. V., Aramova, O. Y., Tishchenko, A. A., Rudoy, D. V. & Chikindas, M. L. RNA stability: a review of the role of structural features and environmental conditions. *Molecules* **29**, 5978 (2024).
65. Mortimer, S. A., Kidwell, M. A. & Doudna, J. A. Insights into RNA structure and function from genome-wide studies. *Nat. Rev. Genet.* **15**, 469–479 (2014).
66. Leppek, K. et al. Combinatorial optimization of mRNA structure, stability, and translation for RNA-based therapeutics. *Nat. Commun.* **13**, 1536 (2022).
67. Yu, G., Zhu, H., Chen, X. & Yang, J. R. Specificity of mRNA folding and its association with evolutionarily adaptive mRNA secondary structures. *Genom. Proteom. Bioinf.* **19**, 882–900 (2021).
68. Ma, L. X., Wang, J., Denny Mark, W. & Dong, Y. W. Hindcasted body temperatures reveal underestimated thermal stress faced by intertidal species. *Glob. Ecol. Biogeogr.* **33**, e13908 (2024).
69. Marshall, D. J., Rezende, E. L., Baharuddin, N., Choi, F. & Helmuth, B. Thermal tolerance and climate warming sensitivity in tropical snails. *Ecol. Evol.* **5**, 5905–5919 (2015).

70. Dong, Y. W. et al. Untangling the roles of microclimate, behaviour and physiological polymorphism in governing vulnerability of intertidal snails to heat stress. *P. Roy. Soc. B Biol. Sci.* **284**, 20162367 (2017).
71. Gaitán-Espitia, J. D., Quintero-Galvis, J. F., Mesas, A. & D'Elía, G. Mitogenomics of southern hemisphere blue mussels (Bivalvia: Pteriomorphia): insights into the evolutionary characteristics of the Mytilus edulis complex. *Sci. Rep.* **6**, 268530 (2016).
72. González, V. L. et al. A phylogenetic backbone for Bivalvia: an RNA-seq approach. *P. Roy. Soc. B -Biol. Sci.* **282**, 1471–2954 (2015).
73. Liu, J., Liu, H. & Zhang, H. Phylogeny and evolutionary radiation of the marine mussels (Bivalvia: Mytilidae) based on mitochondrial and nuclear genes. *Mol. Phylogenet. Evol.* **126**, 233–240 (2018).
74. Streit, K., Geiger, D. L. & Lieb, B. Molecular phylogeny and the geographic origin of Haliotidae traced by hemocyanin sequences. *J. Molluscan Stud.* **72**, 105–110 (2005).
75. Uribe, J. E. et al. A Phylogenomic backbone for gastropod molluscs. *Syst. Biol.* **71**, 1271–1280 (2022).
76. Katoh, K., Misawa, K., Kuma, K. & Miyata, T. MAFFT: a novel method for rapid multiple sequence alignment based on fast Fourier transform. *Nucleic Acids Res.* **30**, 3059–3066 (2002).
77. Price, M. N., Dehal, P. S. & Arkin, A. P. FastTree 2 – Approximately maximum-likelihood trees for large alignments. *PLoS ONE***5**, e9490 (2010).
78. Tamura, K., Stecher, G. & Kumar, S. MEGA11: Molecular evolutionary genetics analysis version 11. *Mol. Biol. Evol.* **38**, 3022–3027 (2021).
79. Keck, F., Rimet, F., Bouchez, A. & Franc, A. phylosignal: an R package to measure, test, and explore the phylogenetic signal. *Ecol. Evol.* **6**, 2774–2780 (2016).
80. Paradis, E., Claude, J. & Strimmer, K. APE: analyses of phylogenetics and evolution in R language. *Bioinformatics* **20**, 289–290 (2004).
81. Orme, D. et al. CAPER: comparative analyses of phylogenetics and evolution in R. *Methods Ecol. Evol.* **3**, 145–151 (2013).
82. Freckleton, R. P., Harvey, P. H. & Pagel, M. Phylogenetic analysis and comparative data: a test and review of evidence. *Am. Nat.* **160**, 712–726 (2002).
83. Dahlhoff, E. A. & Somero, G. N. Kinetic and structural adaptations of cytoplasmic malate dehydrogenases of eastern Pacific abalone (genus *Haliotis*) from different thermal habitats: biochemical correlates of biogeographical patterning. *J. Exp. Biol.* **185**, 137–150 (1993).
84. Fields, P. A., Rudomin, E. L. & Somero, G. N. Temperature sensitivities of cytosolic malate dehydrogenases from native and invasive species of marine mussels (genus *Mytilus*): sequence-function linkages and correlations with biogeographic distribution. *J. Exp. Biol.* **209**, 656–667 (2006).
85. Zhang, Y. I-TASSER server for protein 3D structure prediction. *BMC Bioinform.* **9**, 40 (2008).
86. MacKerell, A. D. Jr. et al. All-atom empirical potential for molecular modeling and dynamics studies of proteins. *J. Phys. Chem. B* **102**, 3586–3616 (1998).
87. MacKerell, A. D. Jr, Feig, M. & Brooks, C. L. Improved treatment of the protein backbone in empirical force fields. *J. Am. Chem. Soc.* **126**, 698–699 (2004).
88. Phillips, J. C. et al. Scalable molecular dynamics with NAMD. *J. Comput. Chem.* **26**, 1781–1802 (2005).
89. Best, R. B. et al. Optimization of the additive CHARMM all-atom protein force field targeting improved sampling of the backbone Φ, Ψ and side-chain X1 and X2 dihedral angles. *J. Chem. Theory Comput.* **8**, 3257–3273 (2012).
90. Humphrey, W., Dalke, A. & Schulten, K. VMD: visual molecular dynamics. *J. Mol. Graph.* **14**, 33–38 (1996).
91. Lorenz, R. et al. ViennaRNA package 2.0. *Algorithms Mol. Biol.* **6**, 26 (2011).
92. Mathews, D. H., Sabina, J., Zuker, M. & Turner, D. H. Expanded sequence dependence of thermodynamic parameters improves prediction of RNA secondary structure. *J. Mol. Biol.* **288**, 911–940 (1999).
93. Zhang, X. L., Liao, M. L. & Dong, Y. W. The simulation input files [Data set]. figshare, https://doi.org/10.6084/m9.figshare.28386131 (2025).


## Acknowledgements

We thank Prof. George Somero of Hopkins Marine Station, Stanford University for his constructive suggestions, discussions, and writing revision. We also thank Qing-Yu Dong and Jia-Rong Liu of College of Marine Life Sciences, Ocean University of China for their guidance of experiment. MDS were conducted on the supercomputer platform of Qingdao Marine Science and Technology Center. This work was kindly supported by National Natural Science Foundation of China (grant numbers 42025604 and 42376102) and the Fundamental Research Funds for the Central Universities.

## Author contributions

X.-L.Z.: investigation, data curation, methodology, writing – original draft; M.-L.L.: methodology, funding acquisition, supervision, writing – original draft, writing – review and editing; C.-Y.M.: data curation, methodology; L.-X.M.: data curation, methodology; Q.-W.H.: investigation; Y.-W.D.: conceptualization, funding acquisition, supervision, writing – review and editing.

## Competing interests

The authors declare no competing interests.

## Additional information

**Supplementary information** The online version contains supplementary material available at https://doi.org/10.1038/s42003-025-07881-8.

**Correspondence** and requests for materials should be addressed to Ming-Ling Liao.

**Peer review information** *Communications Biology* thanks Saurav Mallik and Mahdie Rahban and the other, anonymous, reviewer(s) for their contribution to the peer review of this work. Primary Handling Editors: Linn Hoffmann and Johannes Stortz.